Adaptive Rate Splitting for Uplink Non-Orthogonal Multiple Access Systems

Hongwu Liu* and Kyung Sup Kwak†
*ICDT Innovation Center, Shandong Jiaotong University, Jinan 250357, China
†Department of Information and Communications Engineering, Inha University, Incheon 22212, South Korea

***Abstract*—In this paper, a fixed rate splitting (FRS) scheme and an adaptive rate splitting (ARS) scheme are proposed for an uplink non-orthogonal multiple access (NOMA) system, in which a near user and a far user communicate with a base-station (BS) using power-domain NOMA. Considering back-off power control, information signal of near user is split into two data streams for uplink transmissions, whereas information signal of far user is transmitted without rate splitting. In the FRS scheme, a fixed power allocation factor is applied at near user for allocating transmit power between data streams. At the BS receiver, successive interference cancellation is applied for recovering all data streams. Motivated by cognitive radio principles, a dynamic power allocation factor is designed for the ARS scheme based on instantaneous channel state information. Closed-form expressions are derived for outage probabilities of the near and far users, respectively. In addition, analytical expressions are derived for asymptotic outage probabilities of the FRS and ARS schemes, respectively. The superior outage performance achieved by the FRS and ARS schemes are corroborated by system-level simulation results.**

***Index Terms*—NOMA, rate splitting, outage probability, cognitive radio.**

I. Introduction

Being capable of providing spectral-efficient massive connectivity, non-orthogonal multiple access (NOMA) has been considered as a paradigm shift in multiple access for fifth generation (5G) networks and beyond [1]. With the aid of power-domain superposition coding and successive interference cancellation (SIC), multiple users are served in the same orthogonal resource block along the time, frequency, and/or code axes in power-domain NOMA systems. Under various channel topologies, information theoretic analyses of power-domain NOMA have been widely studied such as those for multiple access channels (MACs) [2], broadcast channels (BCs) [3], interference channels (ICs) [4], and unicast/multicast channels [5], [6]. When channels of far and near users are well separated, it has been shown that power-domain NOMA can achieve superior system performance over that of orthogonal multiple access (OMA) at the cost of that partial users are required to fully decode and cancel interference from other users.

Regarding the capability of delivering different types of service messages to multiple users, rate splitting (RS) techniques have gained a lot of attention recently. In particular, an RS transmitter splits individual information into common and private messages, so that common messages can be decoded by all the receivers. In [7] and [8], it has been shown that RS can achieve the allowed largest rate-region for a two-user IC. Then, the authors of [9] applied RS for a multi-cell network attaining a significant improvement on the achievable rate. Recently, the RS-aided multiple access techniques have been shown for bridging between NOMA and space-division multiple access (SDMA) in the non-orthogonal unicast and multicast channels [5], [6]. Different from the above RS techniques, another RS technique has been applied for avoiding the complicated users grouping in uplink NOMA systems, in which each user's signal was divided into two parts to generate two virtual users, respectively [10].

For uplink NOMA systems, RS is difficult to be implemented due to the complicated power allocation with respect to both the power-domain superposition coding and RS. Also, the performance analysis of RS in uplink NOMA systems is difficult to be conducted due to the complicated system setting. In this paper, we propose a fixed rate splitting (FRS) scheme and an adaptive rate splitting (ARS) scheme for an uplink NOMA system under the back-off power control [11]. With the aid of the back-off power control, the power allocation is performed between the split data streams, so that it can be optimized for decreasing outage probability.

The main contributions of this paper are summarized as follows:

- An FRS scheme is proposed for the uplink NOMA system under the back-off power control. With the fixed power allocation between the split data streams of the near user, the FRS scheme can achieve an improved outage performance over that of conventional NOMA under the back-off power control.
- An ARS scheme is proposed to achieve the allowed minimum outage probability. Regarding the virtual and real users as the primary, secondary, and tertiary users according to their detecting order in the SIC, the dynamic power allocation is implemented in a cognitive way for the data streams, which significantly improves the outage performance of the considered system.
- For both the FRS and ARS schemes, closed-form expressions are derived for the outage probabilities of the near and far users, respectively. Asymptotic outage probability floors are also derived for all the considered schemes. The superior outage performance achieved by the FRS and ARS schemes is verified by system-level simulation results.

The remainder of this paper is organized as follows: Section II presents the system model of the uplink NOMA system under the back-off power control; Section III presents the FRS scheme and provides the corresponding outage performance analysis. Section IV proposes the ARS scheme and presents the corresponding outage performance analysis; Section V presents the simulation results and verifies the enhanced outage performance achieved by the proposed schemes. Section VI summarizes this work.

II. NOMA under Back-off Power Control

We consider an uplink NOMA system consisting of a base station (BS) and a pair of users, U_1 and U_2. Without loss of generality, we assume that U_1 and U_2 are the near and far users, respectively. The channel from U_i ($i = 1$ or 2) to the BS is denoted by h_i, which is modeled as independent but not identically distributed (i.n.i.d.) Rayleigh fading. In addition, a path-loss component $\mathcal{L}_i$ is associated with h_i for representing the large-scale fading. The information signal of U_i is denoted by x_i, which follows independent and identically distributed (i.i.d.) complex Gaussian distribution with zero mean and unit variance.

In each block of transmissions, U_1 and U_2 transmit their information signals to the BS simultaneously. At the BS, the received signal can be expressed as:

$$y = \sqrt{P_1\mathcal{L}_1}h_1x_1 + \sqrt{P_2\mathcal{L}_2}h_2x_2 + n, \tag{1}$$

where P_i is the transmit power of U_i and n is the additive white Gaussian noise (AWGN) at the BS receiver with zero mean and variance σ^2. The BS receiver first detects the near user's signal by treating the far user's signal as noise. Then, the BS receiver applies SIC for detecting the far user's signal. Based on (1), the received signal-to-interference-plus-noise ratio (SINR) and signal-to-noise ratio (SNR) for detecting x_1 and x_2 can be derived as:

$$\gamma_1 = \frac{P_1\mathcal{L}_1|h_1|^2}{P_2\mathcal{L}_2|h_2|^2 + \sigma^2} \tag{2}$$

and

$$\gamma_2 = \frac{P_2\mathcal{L}_2|h_2|^2}{\sigma^2}, \tag{3}$$

respectively. To ensure the diverse power levels of the arrived signals required by the SIC processing, we adopt the back-off power control of [11], i.e., the transmit power of U_i is given by

$$P_i = P_t - (i-1)\tilde{\varepsilon} - 10\log_{10}(\mathcal{L}_i), \tag{4}$$

where P_t is the target arrived power of the received signal at the BS and $\tilde{\varepsilon}$ is the power step level ($\tilde{\varepsilon} \geq 0$ dB). Accordingly, we have a linear relationship $P_2\mathcal{L}_2 = \varepsilon P_1\mathcal{L}_1$ with $\varepsilon \triangleq 10^{-\frac{\tilde{\varepsilon}}{10}}$ satisfying $0 < \varepsilon \leq 1$. Substituting $P_2\mathcal{L}_2 = \varepsilon P_1\mathcal{L}_1$ into (2) and (3), the received SINR and SNR for detecting x_1 and x_2 can be rewritten as:

$$\gamma_1 = \frac{\rho|h_1|^2}{\varepsilon\rho|h_2|^2 + 1} \tag{5}$$

and

$$\gamma_2 = \varepsilon\rho|h_2|^2, \tag{6}$$

respectively, where $\rho \triangleq P_1\mathcal{L}_1/\sigma^2$.

A. Outage Probability Analysis

In this part, the outage probabilities of U_1 and U_2 achieved by the uplink NOMA under the back-off power control are analyzed, respectively. For the user U_i, we denote its targeted transmit rate by $\widehat{R}_i$ with $i = 1$ and 2. Then, the required SINR/SNR threshold for the successful achieving $\widehat{R}_i$ can be expressed as $\widehat{\gamma}_i = 2^{\widehat{R}_i} - 1$.

Since the random variable (RV) $g_i \triangleq \rho|h_i|^2$ follows an exponential distribution with the scale parameter of $\rho\lambda_i$, where $\lambda_i \triangleq \mathbb{E}\{|h_i|^2\}$, the probability density function (PDF) and cumulative distribution function (CDF) of g_i can be respectively expressed as:

$$f_{g_i}(x) = \frac{1}{\rho\lambda_i}e^{-\frac{x}{\rho\lambda_i}} \quad \text{and} \quad F_{g_i}(x) = 1 - e^{-\frac{x}{\rho\lambda_i}}. \tag{7}$$

For the detection of x_1, an outage event occurs if $\gamma_1 < \widehat{\gamma}_1$. For the detection of x_2, the outage events include two cases: 1) $\gamma_1 < \widehat{\gamma}_1$; 2) $(\gamma_1 \geq \widehat{\gamma}_1) \cap (\gamma_2 < \widehat{\gamma}_2)$.

Theorem 1. *The outage probabilities of U_1 and U_2 achieved by the uplink NOMA under the back-off power control are respectively given by*

$$P_{\text{out},1} = 1 - \frac{\lambda_1 e^{-\frac{\widehat{\gamma}_1}{\rho\lambda_1}}}{\lambda_1 + \varepsilon\lambda_2\widehat{\gamma}_1} \tag{8}$$

and

$$P_{\text{out},2} = 1 - \frac{\lambda_1 e^{-\frac{\widehat{\gamma}_2}{\varepsilon\rho\lambda_2} - \frac{\widehat{\gamma}_1(1+\widehat{\gamma}_2)}{\rho\lambda_1}}}{\lambda_1 + \varepsilon\lambda_2\widehat{\gamma}_1}. \tag{9}$$

Proof: With the aid of $f_{g_i}(x)$ and $F_{g_i}(x)$ in (7), the outage probabilities $P_{\text{out},1} = \Pr\{\gamma_1 < \widehat{\gamma}_1\}$ and $P_{\text{out},2} = \Pr\{\gamma_1 < \widehat{\gamma}_1\} + \Pr\{(\gamma_1 \geq \widehat{\gamma}_1) \cap (\gamma_2 < \widehat{\gamma}_2)\}$ can be easily evaluated as (8) and (9), respectively. ■

As $\rho \to \infty$, we have $e^{-\frac{c}{\rho}} \to 1$ for a constant c. Thus, asymptotic outage probabilities of U_1 and U_2 are the same, which is given by

$$P_{\text{out}}^{\infty} = 1 - \frac{\lambda_1}{\lambda_1 + \varepsilon\lambda_2\widehat{\gamma}_1}. \tag{10}$$

III. FRS Scheme

For the uplink NOMA system consisting of two users, we only consider the RS at a single user [12]. Specifically, the RS is applied at the near user in the FRS scheme. Taking into account the back-off power control, a fixed power allocation factor is employed for allocating the transmit power between two data streams of the near user.

For the near user, its information signal x_1 is split into the data streams x_{11} and x_{12}, respectively, which correspond to two virtual users U_{11} and U_{12}, respectively. Accordingly, the received signal at the BS can be written as:

$$y = \sqrt{\alpha\bar{P}_1}h_1x_{11} + \sqrt{(1-\alpha)\bar{P}_1}h_1x_{12} + \sqrt{\bar{P}_2}h_2x_2 + n, \tag{11}$$

where α is the power allocation factor. Considering the three users, U_{11}, U_{12}, and U_2, the detecting orders at the BS can be classified into several kinds [10]. For simplicity, we only consider one kind of the detecting order, i.e., $x_{11} \to x_2 \to x_{12}$. Based on (11), the received SINR for detecting x_{11} can be derived as

$$\gamma_{11} = \frac{\alpha\rho|h_1|^2}{(1-\alpha)\rho|h_1|^2 + \varepsilon\rho|h_2|^2 + 1}. \tag{12}$$

After recovering x_{11} and subtracting the corresponding reconstructed signal from (11), the remaind signal for detecting x_2 can be generated as:

$$y = \sqrt{\bar{P}_2}h_2x_2 + \sqrt{(1-\alpha)\bar{P}_1}h_1x_{12} + n. \tag{13}$$

Thus, the received SINR for detecting x_2 can be derived as:

$$\gamma_2 = \frac{\varepsilon\rho|h_2|^2}{(1-\alpha)\rho|h_1|^2 + 1}. \tag{14}$$

With the aid of the SIC processing, the remained signal for detecting x_{12} is given by

$$y = \sqrt{(1-\alpha)\bar{P}_1}h_1x_{12} + n. \tag{15}$$

and the received SNR for detecting x_{12} can be derived as:

$$\gamma_{12} = (1-\alpha)\rho|h_1|^2. \tag{16}$$

A. Outage Probability Analysis

In this section, the outage probabilities of U_1 and U_2 achieved by the FRS scheme are analyzed, respectively. For the virtual users U_{11} and U_{12}, we denote the corresponding target rates by $\widehat{R}_{11}$ and $\widehat{R}_{12}$, respectively. Then, the required SINR/SNR threshold for the successful achieving $\widehat{R}_j$ can be expressed as $\widehat{\gamma}_j = 2^{\widehat{R}_j} - 1$ with $j \in \{11, 12\}$. Moreover, we have $\widehat{R}_{11} = \beta\widehat{R}_1$ and $\widehat{R}_{12} = (1-\beta)\widehat{R}_1$, where $0 < \beta < 1$ is the target RS factor.

When the detecting order $x_{11} \to x_2 \to x_{12}$ is applied, the outage events of U_1 can be classified into three cases: 1) $\gamma_{11} < \widehat{\gamma}_{11}$; 2) $(\gamma_{11} \geq \widehat{\gamma}_{11}) \cap (\gamma_2 < \widehat{\gamma}_2)$; 3) $(\gamma_{11} \geq \widehat{\gamma}_{11}) \cap (\gamma_2 \geq \widehat{\gamma}_2) \cap (\gamma_{12} < \widehat{\gamma}_{21})$. Accordingly, the outage probability of U_1 can be expressed as:

$$\begin{aligned} P_{\text{out},1} = {} & \Pr\{\gamma_{11} < \widehat{\gamma}_{11}\} + \Pr\{(\gamma_{11} \geq \widehat{\gamma}_{11}) \cap (\gamma_2 < \widehat{\gamma}_2)\} \\ & + \Pr\{(\gamma_{11} \geq \widehat{\gamma}_{11}) \cap (\gamma_2 \geq \widehat{\gamma}_2) \cap (\gamma_{12} < \widehat{\gamma}_{21})\}. \end{aligned} \tag{17}$$

As such, the outage probability of U_2 can be written as:

$$P_{\text{out},2} = \Pr\{\gamma_{11} < \widehat{\gamma}_{11}\} + \Pr\{(\gamma_{11} \geq \widehat{\gamma}_{11}) \cap (\gamma_2 < \widehat{\gamma}_2)\}. \tag{18}$$

Theorem 2. *When the FRS scheme is applied, the outage probabilities of U_1 and U_2 are given by*

$$\begin{aligned} P_{\text{out},1} = {} & 1 - \frac{\varepsilon\lambda_2 e^{-\frac{\tau}{\rho\lambda_1} - \frac{(1+(1-\alpha)\tau)\widehat{\gamma}_2}{\varepsilon\rho\lambda_2}}}{\varepsilon\lambda_2 + (1-\alpha)\lambda_1\widehat{\gamma}_2} \\ & + \frac{\varepsilon\lambda_2\widehat{\gamma}_{11} e^{-\frac{\tau}{\rho\lambda_1} + \frac{\widehat{\gamma}_{11} - (\alpha - (1-\alpha)\widehat{\gamma}_{11})\tau}{\varepsilon\rho\lambda_2\widehat{\gamma}_{11}}}}{\alpha\lambda_1 - ((1-\alpha)\lambda_1 - \varepsilon\lambda_2)\widehat{\gamma}_{11}} \end{aligned} \tag{19}$$

and

$$\begin{aligned} P_{\text{out},2} = {} & 1 - \frac{\varepsilon\lambda_2 e^{-\frac{\tau_3}{\rho\lambda_1} - \frac{(1+(1-\alpha)\tau_3)\widehat{\gamma}_2}{\varepsilon\rho\lambda_2}}}{\varepsilon\lambda_2 + (1-\alpha)\lambda_1\widehat{\gamma}_2} \\ & + \frac{\varepsilon\lambda_2\widehat{\gamma}_{11} e^{-\frac{\tau_3}{\rho\lambda_1} + \frac{\widehat{\gamma}_{11} - (\alpha - (1-\alpha)\widehat{\gamma}_{11})\tau_3}{\varepsilon\rho\lambda_2\widehat{\gamma}_{11}}}}{\alpha\lambda_1 - ((1-\alpha)\lambda_1 - \varepsilon\lambda_2)\widehat{\gamma}_{11}}, \end{aligned} \tag{20}$$

respectively, where $\tau \triangleq \max\{\tau_1, \tau_2, \tau_3\}$, $\tau_1 \triangleq \frac{\widehat{\gamma}_{12}}{1-\alpha}$, $\tau_2 \triangleq \frac{\widehat{\gamma}_{11}}{\alpha - (1-\alpha)\widehat{\gamma}_{11}}$, *and* $\tau_3 \triangleq \frac{(1+\widehat{\gamma}_2)\widehat{\gamma}_{11}}{\alpha - (1-\alpha)(1+\widehat{\gamma}_2)\widehat{\gamma}_{11}}$.

Proof: See Appendix A. ∎

The above results characterize the outage performance of U_1 and U_2 in terms of the transmit SNR, power allocation factor, and target RS rates, which can be easily evaluated by computer computation. Besides, it is shown that the outage probabilities of U_1 and U_2 are correlated with each other via the target rates $\widehat{R}_1$ and $\widehat{R}_2$, respectively. Based on (19) and (20), as $\rho \to \infty$, asymptotic outage probabilities of U_1 and U_2 achieved by the FRS scheme are the same, which is given by

$$\begin{aligned} P_{\text{out}}^{\infty} = {} & 1 - \frac{\varepsilon\lambda_2}{\varepsilon\lambda_2 + (1-\alpha)\lambda_1\widehat{\gamma}_2} \\ & + \frac{\varepsilon\lambda_2\widehat{\gamma}_{11}}{\alpha\lambda_1 - ((1-\alpha)\lambda_1 - \varepsilon\lambda_2)\widehat{\gamma}_{11}}. \end{aligned} \tag{21}$$

IV. ARS Scheme

Motivated by the fact that NOMA can be treated as a special case of cognitive radio systems [13], we propose the ARS scheme in this section.

When the detecting order $x_{11} \to x_2 \to x_{12}$ is applied at the BS for the SIC processing, U_{11}, U_2, and U_{12} are treated as the primary, secondary, and tertiary users, respectively. Obviously, an unsuccessful detection of x_{12} or x_2 results in an incorrect detecting of x_{12}, which in turn results in an outage transmission of x_1 for U_1. In addition, an unsuccessful detection of x_{11} results in an outage transmission of x_2 for U_2. In the ARS scheme, the power allocation factor is designed with the priority for satisfying the quality of service (QoS) requirements of U_{11}, U_2, and U_{12} sequentially.

For the successful detecting of x_{11}, the QoS requirement $\gamma_{11} \geq \widehat{\gamma}_{11}$ can be rewritten as:

$$\alpha \in [\widehat{\alpha}, 1], \quad \text{subject to} \quad \widehat{\gamma}_{11} \leq \frac{g_1}{1 + \varepsilon g_2}, \tag{22}$$

where

$$\widehat{\alpha} = \frac{\widehat{\gamma}_{11}}{1 + \widehat{\gamma}_{11}}\left(1 + \frac{1}{g_1} + \frac{\varepsilon g_2}{g_1}\right) \tag{23}$$

is the minimum value of α satisfying $\gamma_{11} \geq \widehat{\gamma}_{11}$ and the constraint $\widehat{\gamma}_{11} \leq \frac{g_1}{1+\varepsilon g_2}$ is applied to restrict $0 < \widehat{\alpha}_1 \leq 1$. For the successful detecting of x_2, the QoS requirement $\gamma_2 \geq \widehat{\gamma}_2$ can be rewritten as:

$$\alpha \in [\widetilde{\alpha}, 1], \quad \text{subject to} \quad \widehat{\gamma}_2 \leq \varepsilon g_2, \tag{24}$$

where

$$\widetilde{\alpha} = \max\left(0, 1 + \frac{1}{g_1} - \frac{\varepsilon g_2}{\widehat{\gamma}_2 g_1}\right) \tag{25}$$

is the minimum value of α satisfying $\gamma_2 \geq \widehat{\gamma}_2$ and the constraint $\widehat{\gamma}_2 \leq \varepsilon g_2$ is applied to restrict $\widetilde{\alpha} \leq 1$. Then, the power allocation factor satisfying both $\gamma_{11} \geq \widehat{\gamma}_{11}$ and $\gamma_2 \geq \widehat{\gamma}_2$ is constrained by

$$\alpha \in \begin{cases} [\max(\widehat{\alpha}, \widetilde{\alpha}), 1], & \widehat{\gamma}_{11} \leq \frac{g_1}{1+\varepsilon g_2} \text{ and } \widehat{\gamma}_2 \leq \varepsilon g_2, \\ \text{does not exist}, & \text{otherwise}. \end{cases} \tag{26}$$

Corresponding to the detection of x_{12}, to achieve a probability $\Pr\{\gamma_{12} \geq \widehat{\gamma}_{12}\}$ as large as possible considering that γ_{12} decreases monotonically with increasing α, the power allocation factor needs to be minimized besides the constraint (26). Therefore, the power allocation factor of the ARS scheme is given by

$$\alpha = \begin{cases} \max(\widehat{\alpha}, \widetilde{\alpha}), & \widehat{\gamma}_{11} \leq \frac{g_1}{1+\varepsilon g_2} \text{ and } \widehat{\gamma}_2 \leq \varepsilon g_2, \\ \text{does not exist}, & \text{otherwise}. \end{cases} \tag{27}$$

Based on (27), a non-outage event of detecting x_1 occurs if α exists and the corresponding γ_{12} is required to satisfy $\gamma_{12}(\alpha) \geq \widehat{\gamma}_{12}$, where $\gamma_{12}(\alpha)$ is a function of α given by (16). Since there are two possible values for a feasible α according to (27), the outage probability of U_1 can be expressed as:

$$\begin{aligned} P_{\text{out},1} = 1 &- \Pr\Big\{\big(\widehat{\gamma}_{11} \leq \tfrac{g_1}{1+\varepsilon g_2}\big) \cap \big(\widehat{\gamma}_2 \leq \varepsilon g_2\big) \\ &\cap \big(\widehat{\alpha} \geq \widetilde{\alpha}\big) \cap \big(\gamma_{12}(\widehat{\alpha}) \geq \widehat{\gamma}_{12}\big)\Big\} \\ &- \Pr\Big\{\big(\widehat{\gamma}_{11} \leq \tfrac{g_1}{1+\varepsilon g_2}\big) \cap \big(\widehat{\gamma}_2 \leq \varepsilon g_2\big) \\ &\cap \big(\widehat{\alpha} < \widetilde{\alpha}\big) \cap \big(\gamma_{12}(\widetilde{\alpha}) \geq \widehat{\gamma}_{12}\big)\Big\}. \end{aligned} \tag{28}$$

As such, the outage probability of U_2 can be expressed as:

$$P_{\text{out},2} = 1 - \Pr\Big\{\big(\widehat{\gamma}_{11} \leq \tfrac{g_1}{1+\varepsilon g_2}\big) \cap \big(\widehat{\gamma}_2 \leq \varepsilon g_2\big)\Big\}. \tag{29}$$

Theorem 3. *The outage probabilities of U_1 and U_2 achieved by the ARS scheme are given by*

$$\begin{aligned} P_{\text{out},1} = 1 &- \frac{\lambda_1}{\lambda_1 + \varepsilon\lambda_2\widehat{\gamma}_{11}} \\ &\times e^{-\frac{1}{\rho}\left(\frac{\widehat{\gamma}_2(1+\widehat{\gamma}_{12})}{\varepsilon\lambda_2} + \frac{\widehat{\gamma}_{12}+\widehat{\gamma}_{11}(1+\widehat{\gamma}_{12})(\widehat{\gamma}_2)}{\lambda_1}\right)} \end{aligned} \tag{30}$$

and

$$P_{\text{out},2} = 1 - \frac{\lambda_1}{\lambda_1 + \varepsilon\lambda_2\widehat{\gamma}_{11}} e^{-\frac{1}{\rho}\left(\frac{\widehat{\gamma}_{11}(1+\widehat{\gamma}_2)}{\lambda_1} + \frac{\widehat{\gamma}_2}{\varepsilon\lambda_2}\right)}, \tag{31}$$

respectively.

Proof: See Appendix B. ∎

As $\rho \to \infty$, we have $e^{-\frac{c}{\rho}} \to 1$ for a constant c. Thus, asymptotic outage probabilities of U_1 and U_2 achieved by the ARS scheme are the same, which is given by

$$P_{\text{out}}^{\infty} = 1 - \frac{\lambda_1}{\lambda_1 + \varepsilon\lambda_2\widehat{\gamma}_{11}}. \tag{32}$$

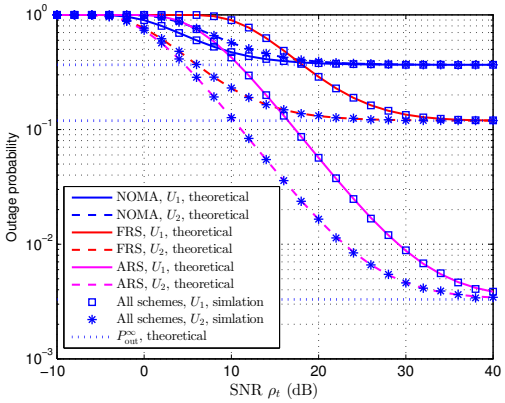

Fig. 1. Outage probability versus target arrived SNR ρ_t.

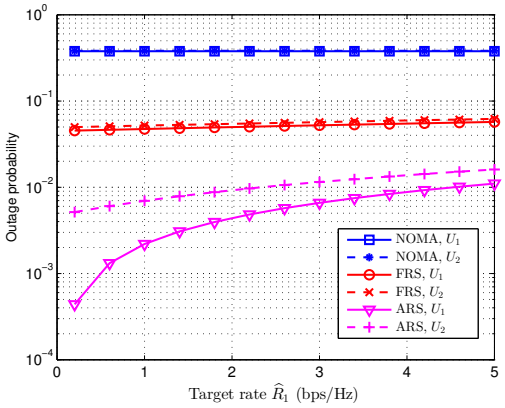

Fig. 2. Outage probability versus $\widehat{R}_1$ (fixed $\widehat{R}_2 = 0.2$ bps/Hz).

V. Simulation Results

In this section, we present system level simulation results to verify the superior outage performance achieved by the FRS and ARS schemes, respectively. In the system-level simulation [14], we assume the distances from the BS to the near and far users are 50 meters and 100 meters, respectively, and set the large-scale fading $\mathcal{L}_i$ as that of [11]. In addition, the target arrived SNR is defined as $\rho_t = P_t/\sigma^2$.

The outage probability versus target arrived SNR is investigated in Fig. 1, in which we set $\widehat{R}_1 = 1.5$ bps/Hz, $\widehat{R}_2 = 0.5$ bps/Hz, $\tilde{\varepsilon} = 5$ dB, and $\beta = 0.01$. In addition, we set $\alpha = 0.9$ for the FRS scheme. The results in Fig. 1 show that both the FRS and ARS schemes decrease the outage probabilities for U_1 and U_2, respectively, as ρ_t increases. Although the FRS and ARS schemes achieve the higher outage probabilities for U_1 in the low and middle SNR regions than that of the back-off power control-aided NOMA without employing RS (denoted as "NOMA" in Fig. 2), the proposed two RS schemes achieve the smaller outage probabilities in the high SNR region. For U_2, both the FRS and ARS schemes achieve the smaller outage probabilities than those of "NOMA" in the considered whole SNR region. In addition, the ARS scheme achieves the smaller outage probabilities than those of the FRS scheme in the considered whole SNR region. The results in Fig. 1 also

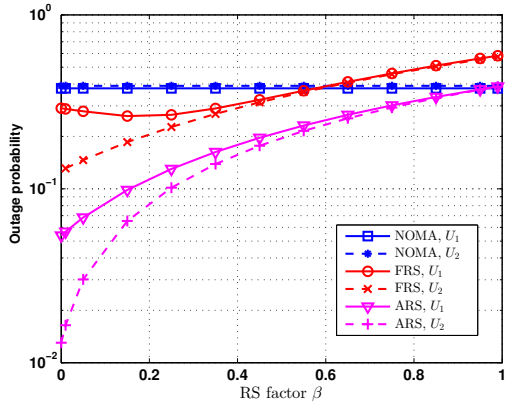

Fig. 3. Outage probability versus target RS factor β.

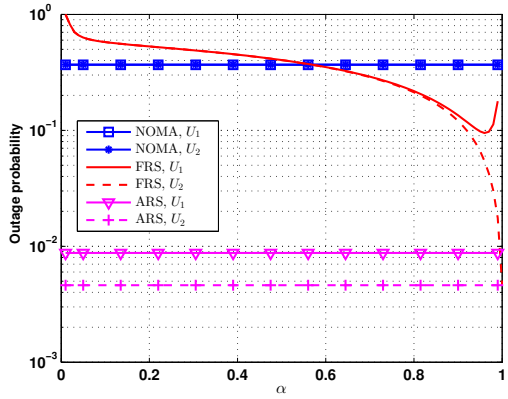

Fig. 4. Outage probability versus power allocation factor α.

verify the correctness of the derived analytical results. In the high SNR region, the outage probabilities of both two users approach the same floor as predicted by the analytical results. Moreover, the ARS scheme achieves the smallest floor for the outage probabilities among all the considered schemes.

In Fig. 2, we investigate the impact of the target rates on the outage probability, where we set $\rho_t = 20$ dB, $\beta = 0.01$, $\tilde{\varepsilon} = 5$ dB, and a fixed $\widehat{R}_2 = 0.2$ bps/Hz. As it is shown in Fig. 2, the FRS and ARS schemes achieve the smaller outage probabilities than those of "NOMA" in the considered whole $\widehat{R}_1$ region. Among all the schemes, the ARS scheme achieves the smallest outage probabilities for both U_1 and U_2 in the considered whole $\widehat{R}_1$ region. As $\widehat{R}_1$ increases, the outage probabilities achieved by the ARS scheme also increase for U_1 and U_2, respectively. In contrary, the outage probabilities achieved by "NOMA" keep almost the same as $\widehat{R}_1$ increases.

The impact of the target RS factor β on the outage probability is investigated in Fig. 3, where we set $\rho_t = 20$ dB, $\widehat{R}_1 = 1.5$ bps/Hz, $\widehat{R}_2 = 0.5$ bps/Hz, and $\tilde{\varepsilon} = 5$ dB. For the FRS scheme, we set $\alpha = 0.9$. The results in Fig. 3 show that the ARS scheme achieves the smallest outage probabilities for U_1 and U_2, respectively, in the considered whole β region. For the FRS scheme, the outage probabilities of U_1 and U_2 are smaller than those of "NOMA" in the small and middle β regions. However, in the large β region, the outage probabilities of U_1 and U_2 achieved by the FRS scheme are larger than those of "NOMA". As β increases, the outage probabilities of U_1 and U_2 achieved by the ARS scheme also increase and this tendency also occurs for the outage probability of U_2 achieved by the FRS scheme. However, the outage probability of U_1 achieved by the FRS scheme first decreases with increasing β and then increases with increasing β after β surpasses a threshold value.

In Fig. 4, we investigate the impact of the power allocation factor on the outage performance of the FRS scheme along with outage performance comparison for all the considered schemes. In Fig. 4, we set $\widehat{R}_1 = 1.5$ bps/Hz, $\widehat{R}_2 = 0.5$ bps/Hz, $\beta = 0.1$, $\tilde{\varepsilon} = 5$ dB, and $\rho_t = 30$ dB. The results in Fig. 4 show that the power allocation factor has different effects on the outage probabilities of U_1 and U_2 when the FRS scheme is applied. For U_1, the outage probability first decreases with increasing α; then, the outage probability increases with increasing α after α approaches a threshold value. For U_2, the outage probability always decreases with increasing α. For the FRS scheme, the outage probabilities of U_1 and U_2 are smaller than those of "NOMA" in the large α region, which suggests that α should be set with a large value for the FRS scheme. Moreover, the ARS scheme achieves the smallest outage probabilities for both U_1 and U_2 among all the schemes.

VI. Conclusions

In this paper, FRS and ARS schemes have been proposed for the uplink NOMA system under back-off power control. It has been shown that the proposed RS schemes can significantly improve the outage performance for the paired two users. Closed-form expressions for the outage probabilities of both users have been derived for the FRS and ARS schemes, respectively. Asymptotic outage probabilities have been presented for all the considered schemes. For the proposed FRS and ARS schemes, the achieved superior outage performance have been verified by Monte Carlo simulation results.

Acknowledgement

This research is supported by the MSIT (Ministry of Science, ICT), Korea, under the ITRC support program (IITP-2018-2014-1-00729) supervised by the IITP.

Appendix A: A proof of Theorem 2

For detecting x_1, a non-outage event occurs only when $\gamma_{11} \geq \widehat{\gamma}_{11}$, $\gamma_2 \geq \widehat{\gamma}_2$, and $\gamma_{12} \geq \widehat{\gamma}_{12}$ happen simultaneously, i.e., x_{11}, x_2, and x_{12} are correctly detected. Let $I_1 \triangleq \Pr\{(\gamma_{11} \geq \widehat{\gamma}_{11}) \cap (\gamma_2 \geq \widehat{\gamma}_2) \cap (\gamma_{12} \geq \widehat{\gamma}_{12})\}$, the outage probability in (17) can be rewritten as: $P_{\text{out},1} = 1 - I_1$. After some mathematical manipulation, the term I_1 can be rewritten as:

$$I_1 = \Pr\left\{(g_1 \geq \tau) \cap \left(\frac{\widehat{\gamma}_2 + (1-\alpha)\widehat{\gamma}_2 g_1}{\varepsilon} < g_2 < \frac{(\alpha - (1-\alpha)\widehat{\gamma}_{11})g_1 - \widehat{\gamma}_{11}}{\varepsilon \widehat{\gamma}_{11}}\right)\right\}, \quad (33)$$

where $\tau \triangleq \max\{\tau_1, \tau_2, \tau_3\}$, $\tau_1 \triangleq \frac{\widehat{\gamma}_{12}}{1-\alpha}$, $\tau_2 \triangleq \frac{\widehat{\gamma}_{11}}{\alpha-(1-\alpha)\widehat{\gamma}_{11}}$, and $\tau_3 \triangleq \frac{(1+\widehat{\gamma}_2)\widehat{\gamma}_{11}}{\alpha-(1-\alpha)(1+\widehat{\gamma}_2)\widehat{\gamma}_{11}}$. Then, I_1 can be evaluated as:

$$\begin{aligned} I_1 &= \int_{\tau}^{\infty} \Big[F_{g_2}\Big(\tfrac{(\alpha-(1-\alpha)\widehat{\gamma}_{11})x-\widehat{\gamma}_{11}}{\varepsilon\widehat{\gamma}_{11}}\Big) \\ &\quad - F_{g_2}\Big(\tfrac{\widehat{\gamma}_2+(1-\alpha)\widehat{\gamma}_2 x}{\varepsilon}\Big)\Big] f_{g_1}(x)\mathrm{d}x \\ &= \frac{\varepsilon\lambda_2 e^{-\frac{\tau}{\rho\lambda_1}-\frac{(1+(1-\alpha)\tau)\widehat{\gamma}_2}{\varepsilon\rho\lambda_2}}}{\varepsilon\lambda_2+(1-\alpha)\lambda_1\widehat{\gamma}_2} \\ &\quad - \frac{\varepsilon\lambda_2\widehat{\gamma}_{11} e^{-\frac{\tau}{\rho\lambda_1}+\frac{\widehat{\gamma}_{11}-(\alpha-(1-\alpha)\widehat{\gamma}_{11})\tau}{\varepsilon\rho\lambda_2\widehat{\gamma}_{11}}}}{\alpha\lambda_1-((1-\alpha)\lambda_1-\varepsilon\lambda_2)\widehat{\gamma}_{11}}. \end{aligned} \tag{34}$$

Substituting (34) into $P_{\mathrm{out},1} = 1 - I_1$, we arrive at (19).

For detecting x_2, a non-outage event occurs only when $\gamma_{11} \geq \widehat{\gamma}_{11}$ and $\gamma_2 \geq \widehat{\gamma}_2$ happen simultaneously, i.e., x_{11} and x_2 are correctly detected. Let $I_2 \triangleq \Pr\{(\gamma_{11} \geq \widehat{\gamma}_{11}) \cap (\gamma_2 \geq \widehat{\gamma}_2)\}$, the outage probability in (18) can be rewritten as: $P_{\mathrm{out},2} = 1 - I_2$. After some mathematical manipulation, the term I_2 can be rewritten as:

$$\begin{aligned} I_2 = \Pr\Big\{ &(g_1 \geq \tau_3) \cap \\ &\Big(\tfrac{\widehat{\gamma}_2+(1-\alpha)\widehat{\gamma}_2 g_1}{\varepsilon} < g_2 < \tfrac{(\alpha-(1-\alpha)\widehat{\gamma}_{11})g_1-\widehat{\gamma}_{11}}{\varepsilon\widehat{\gamma}_{11}}\Big)\Big\}, \end{aligned} \tag{35}$$

which has a similar form as that of I_1 in (33). As such, the outage probability $P_{\mathrm{out},2}$ can be derived as (20).

Appendix B: A proof of Theorem 3

Let $I_3 \triangleq \Pr\Big\{\big(\widehat{\gamma}_{11} \leq \frac{g_1}{1+\varepsilon g_2}\big) \cap \big(\widehat{\gamma}_2 \leq \varepsilon g_2\big) \cap \big(\widehat{\alpha} \geq \widetilde{\alpha}\big) \cap \big(\gamma_{12}(\widehat{\alpha}) \geq \widehat{\gamma}_{12}\big)\Big\}$ and $I_4 \triangleq \Pr\Big\{\big(\widehat{\gamma}_{11} \leq \frac{g_1}{1+\varepsilon g_2}\big) \cap \big(\widehat{\gamma}_2 \leq \varepsilon g_2\big) \cap \big(\widehat{\alpha} < \widetilde{\alpha}\big) \cap \big(\gamma_{12}(\widetilde{\alpha}) \geq \widehat{\gamma}_{12}\big)\Big\}$, the outage probability of U_1 in (28) can be rewritten as $P_{\mathrm{out},1} = 1 - (I_3 + I_4)$.

After some mathematical manipulation, the term I_3 can be expressed as:

$$\begin{aligned} I_3 = \Pr\Big\{ &\Big(g_2 \geq \tfrac{\widehat{\gamma}_2(1+\widehat{\gamma}_{12})}{\varepsilon}\Big) \cap \Big(\varepsilon\widehat{\gamma}_{11}g_2+\widehat{\gamma}_{11}+\widehat{\gamma}_{12}+\widehat{\gamma}_{11}\widehat{\gamma}_{12} \\ &< g_1 < \tfrac{\varepsilon g_2(1+\widehat{\gamma}_{11}+\widehat{\gamma}_{11}\widehat{\gamma}_{12})-\widehat{\gamma}_2}{\widehat{\gamma}_2}\Big)\Big\}. \end{aligned} \tag{36}$$

As such, the term I_4 can be expressed as:

$$\begin{aligned} I_4 = \Pr\Big\{ &\Big(g_2 \geq \tfrac{\widehat{\gamma}_2(1+\widehat{\gamma}_{12})}{\varepsilon}\Big) \cap \\ &\Big(g_1 > \tfrac{\varepsilon g_2(1+\widehat{\gamma}_{11}+\widehat{\gamma}_{11}\widehat{\gamma}_{12})-\widehat{\gamma}_2}{\widehat{\gamma}_2}\Big)\Big\}. \end{aligned} \tag{37}$$

Then, $I_3 + I_4$ can be evaluated as:

$$\begin{aligned} I_3 + I_4 &= \Pr\Big\{\Big(g_2 \geq \tfrac{\widehat{\gamma}_2(1+\widehat{\gamma}_{12})}{\varepsilon}\Big) \cap \\ &\quad \Big(g_1 > \varepsilon\widehat{\gamma}_{11}g_2+\widehat{\gamma}_{11}+\widehat{\gamma}_{12}+\widehat{\gamma}_{11}\widehat{\gamma}_{12}\Big) \\ &= \int_{\frac{\widehat{\gamma}_2(1+\widehat{\gamma}_{12})}{\varepsilon}}^{\infty} \Big[1 - \\ &\quad F_{g_1}\big(\varepsilon\widehat{\gamma}_{11}x+\widehat{\gamma}_{11}+\widehat{\gamma}_{12}+\widehat{\gamma}_{11}\widehat{\gamma}_{12}\big)\Big] f_{g_2}(x)\mathrm{d}x \\ &= \frac{\lambda_1}{\lambda_1+\varepsilon\lambda_2\widehat{\gamma}_{11}} \\ &\quad \times e^{-\frac{1}{\rho}\left(\frac{\widehat{\gamma}_2(1+\widehat{\gamma}_{12})}{\varepsilon\lambda_2}+\frac{\widehat{\gamma}_{12}+\widehat{\gamma}_{11}(1+\widehat{\gamma}_{12})(\widehat{\gamma}_2)}{\lambda_1}\right)}. \end{aligned} \tag{38}$$

Substituting (38) into $P_{\mathrm{out},1} = 1-(I_3+I_4)$, we arrive at (30).

The outage probability $P_{\mathrm{out},2}$ in (29) can be evaluated as:

$$\begin{aligned} P_{\mathrm{out},2} &= 1 - \Pr\Big\{\big(g_2 \geq \tfrac{\widehat{\gamma}_2}{\varepsilon}\big) \cap \big(g_1 > \widehat{\gamma}_{11}(1+\varepsilon g_2)\big)\Big\} \\ &= 1 - \int_{\frac{\widehat{\gamma}_2}{\varepsilon}}^{\infty} \Big(1 - F_{g_1}(1+\varepsilon x)\Big) f_{g_2}(x)\mathrm{d}x \\ &= 1 - \frac{\lambda_1}{\lambda_1+\varepsilon\lambda_2\widehat{\gamma}_{11}} e^{-\frac{1}{\rho}\left(\frac{\widehat{\gamma}_{11}(1+\widehat{\gamma}_2)}{\lambda_1}+\frac{\widehat{\gamma}_2}{\varepsilon\lambda_2}\right)}. \end{aligned} \tag{39}$$

References

[1] Y. Liu, Z. Qin, M. Elkashlan, Z. Ding, A. Nallanathan, and L. Hanzo, "Non-orthogonal multiple access for 5G and beyond," *Proc. IEEE*, vol. 105, no. 12, pp. 2347–2381, Dec. 2017.

[2] D. N. C. Tse and S. V. Hanly, "Multiaccess fading channels. i. polymatroid structure, optimal resource allocation and throughput capacities," *IEEE Trans. Inf. Theory*, vol. 44, no. 7, pp. 2796–2815, Nov. 1998.

[3] T. Cover, "Comments on broadcast channels," *IEEE Trans. Inf. Theory*, vol. 44, no. 6, pp. 2524–2530, Oct. 1998.

[4] T. S. Han and K. Kobayashi, "A new achievable rate region for the interference channel," *IEEE Trans. Inf. Theory*, vol. 27, no. 1, pp. 49–60, Jan. 1981.

[5] B. Clerckx, H. Joudeh, C. Hao, M. Dai, and B. Rassouli, "Rate splitting for mimo wireless networks: a promising PHY-layer strategy for LTE evolution," *IEEE Commun. Mag.*, vol. 54, no. 5, pp. 98–105, May 2016.

[6] Y. Mao, B. Clerckx, and V. O. K. Li, "Rate-splitting for multi-antenna non-orthogonal unicast and multicast transmission," in *Proc. IEEE 19th SPAWC*, Kalamata, Greece, 25-28 Jun. 2018, pp. 1–5.

[7] T. Han and K. Kobayashi, "A new achievable rate region for the interference channel," *IEEE Trans. Inf. Theory*, vol. 27, no. 1, pp. 49–60, Jan. 1981.

[8] R. H. Etkin, D. N. C. Tse, and H. Wang, "Gaussian interference channel capacity to within one bit," *IEEE Trans. Inf. Theory,*, vol. 54, no. 12, pp. 5534–5562, Dec. 2008.

[9] H. Dahrouj and W. Yu, "Multicell interference mitigation with joint beamforming and common message decoding," *IEEE Trans. Commun.*, vol. 59, no. 8, pp. 2264–2273, Aug. 2011.

[10] Y. Zhu, X. Wang, Z. Zhang, X. Chen, and Y. Chen, "A rate-splitting non-orthogonal multiple access scheme for uplink transmission," in *Proc. 9th WCSP*, Nanjing, China, 11-13 Oct. 2017, pp. 1–6.

[11] N. Zhang, J. wang, G. Kang, and Y. Liu, "Uplink non-orthogonal multiple access in 5G systems," *IEEE Communi. Lett.*, vol. 20, no. 3, pp. 458–461, Mar. 2016.

[12] B. Rimoldi and R. Urbanke, "A rate-splitting approach to the Gaussian multiple-access channel," *IEEE Trans. Inf. Theory*, vol. 42, no. 2, pp. 364–375, Mar. 1996.

[13] Z. Ding, P. Fan, and H. V. Poor, "Impact of user pairing on 5G nonorthogonal multiple-access downlink transmissions," *IEEE Trans. Veh. Technol.*, vol. 65, no. 8, pp. 6010–6023, Aug. 2016.

[14] L. Chen, W. Chen, B. Wang, X. Zhang, H. Chen, and D. Yang, "System-level simulation methodology and platform for mobile cellular systems," *IEEE Commun. Mag.*, vol. 49, no. 7, pp. 148–155, Jul. 2011.